Nano-TiO$_2$ for Solar Cells and Photocatalytic Water Splitting: Scientific and Technological Challenges for Commercialization

Marie-Isabelle Baraton*

Centre Européen de la Céramique, SPCTS-UMR CNRS 6638, 12 rue Atlantis, 87068 Limoges, France

Abstract: Nanosized titanium dioxide (nano-TiO$_2$) particles are used in diverse products and devices, including photocatalytic water splitting and solar cells whose successful commercialization is still facing scientific and technological challenges.

Particularly, dye-sensitized solar cells (DSSCs) have recently attracted a lot of attention. The number of papers and patents published in this area has grown exponentially over the last ten years. However, at the present, commercial devices are of small sizes and produced in limited quantities, thus addressing niche markets. Research efforts have largely focused on the optimization of the dye, but the TiO$_2$ nanocrystalline electrode itself also needs to be optimized. It has been shown that particle size and shape, crystallinity, surface morphology and chemistry of the TiO$_2$ material are key parameters to be controlled for enhanced performance of the cell. This article gives an overview of the state-of-the-art on nano-TiO$_2$ for applications in photocatalytic water splitting and, more specifically, in DSSCs. After a brief analysis of the commercial perspectives of DSSCs and of the remaining challenges for their successful commercialization, our approach to the control of the nano-TiO$_2$ surface chemistry for improvement of the DSSC performance is briefly introduced.

1. INTRODUCTION TO TITANIUM OXIDE

The commercial exploitation of titanium dioxide or titania (TiO$_2$) started at the beginning of the 20th century and rapidly increased after the discovery of the sulfate process in 1916 by the Norwegian chemists Farup and Jebsen, and then of the chloride process which was introduced commercially by DuPont in 1958 [1].

1.1. Properties and Applications

Pure titanium dioxide is colorless in the massive state, non-toxic, thermally stable, inert versus acids, alkalis and solvents, and insoluble. It exists under three fundamental crystalline phases: rutile which is the most stable and the most abundant form, anatase (octahedrite) and brookite. All three forms occur naturally but the latter is rather rare and has no commercial interest.

Because of its high refractive index (n=2.54 for anatase or 2.75 for rutile at λ = 550 nm) [2], the main use of TiO$_2$ is as white powder pigment. A relatively low level of TiO$_2$ is needed to achieve a white opaque coating which is resistant to discoloration under ultraviolet (UV) light. TiO$_2$ pigment is used in many diverse products, such as paints, coatings, glazes, enamels, plastics, papers, inks, fibers, foods, pharmaceuticals or cosmetics. As of today, there is no cost-effective alternative to TiO$_2$ pigment [3].

In addition, TiO$_2$ is a photocatalyst and is even considered as the most efficient and environmentally benign photocatalyst [4-7]. As such, it is widely used for the photodegradation of pollutants. Under UV light, water is converted to hydrogen gas by photocatalytic water splitting on a TiO$_2$ electrode [8]. Because of the strong oxidative properties of TiO$_2$ under UV light, this material is used for sterilizing, deodorizing and anti-fouling [5]. Besides, when irradiated with UV light, TiO$_2$ becomes increasingly hydrophilic and can be used for anti-fogging coatings and self-cleaning windows [9-10]. TiO$_2$ is a semiconductor and its electrical properties find applications as gas sensors, especially for humidity and oxygen detection (lambda probes in car engines) (see for example [4]).

1.2. Market

The dominant application of TiO$_2$ is, by far, pigment manufacturing and nearly 95% of the TiO$_2$ production is supplied into the pigment industry with a sales value around US\$ 9 billion for a volume of 4.5 million tons [11]. At the end of 2010, TiO$_2$ traded € 2.60-2.75/kg on the European market and US\$ 1.30-1.44/lb (US\$ 2.87-3.17/kg) on the North-American market [3].

As the major consuming industries of TiO$_2$ are in mature sectors, the global economy has a major impact on the TiO$_2$ industry. Growth in GDP (Gross Domestic Product) usually leads to higher TiO$_2$ demand and vice versa. According to the UK consultant Artikol [12], the global demand growth for TiO$_2$ is estimated to average 2.7% per year until 2019. Growth will be driven by China which is estimated to grow at 5% per year. A lot of potential is also seen in India within the next 10 years.

*Address correspondence to this author at the Centre Européen de la Céramique, SPCTS-UMR CNRS 6638, 12 rue Atlantis, 87068 Limoges France; Tel: +33 680 63 2031; Fax: +33 555 77 8100; E-mail: m-isabelle.baraton@unilim.fr

2. INTRODUCTION TO NANOSIZED TITANIUM DIOXIDE

Nanoscale materials exhibit a much greater surface area for a given mass or volume compared to conventional particles. Therefore, all applications involving surfaces and interfaces will benefit from nanosized particles, enhancing catalytic reactions and increasing interactions with surrounding media. In addition, new physical and chemical properties emerge when the size of the material is reduced to the nanometer scale, leading to quantum confinement effects, affecting the charge transport or causing band gap energy shifts [13, 14 and refs within].

2.1. Specific Properties and Applications

Nanocrystalline TiO_2 usually exhibits a wider band gap than that of the bulk (3.03 eV for rutile and 3.20 eV for anatase) [14]. Moreover, anatase becomes more stable than rutile when the particle size is decreased below 14 nm [15-16]. Generally speaking, the functional properties of nano-TiO_2 are influenced by a large number of factors which include particle size, surface area, synthesis method and conditions, and crystallinity [17].

All the specific properties of nanosized particles have led to the exploitation of nano-TiO_2 for a wide variety of applications in which nano-TiO_2 is essentially preferred over conventional TiO_2 particles. Such applications include self-cleaning surfaces and textiles, UV-resistant coatings and paints, disinfectant sprays, sunscreens, water treatment agents, anticancer treatments (see for example [5, 18, 19]). To date, TiO_2 is indeed one of the most widely used nanoscale materials.

Amongst the multiple uses of nano-TiO_2, two major applications can be highlighted in the field of clean energy, namely photocatalytic water splitting and solar cells. Photocatalytic water splitting into H_2 and O_2 using nanostructured TiO_2 electrodes is thoroughly investigated as it is an environmentally friendly way to produce hydrogen. Another promising application of the TiO_2 semiconductivity is as electrode in dye-sensitized solar cells (DSSCs) in which the high surface-to-volume ratio of the nanostructured semiconductor is required to obtain an acceptable power conversion efficiency [20] (see section 4.2).

2.2. Market

According to Nanoposts.com, a nanotechnology consulting company [21], the commercial potential of nanoscale TiO_2 coatings is important and includes medical applications, architectural (façade paints, wall paper, tiles, consumer goods, cultural heritage, etc.), automotive (anti-fogging glass and mirrors), food and textile industries, environmental protection (water and air purification and disinfection). Besides, the commercialization of nano-TiO_2 photocatalytic material is a potentially lucrative area [21]. Yet, it has to be noted that the total world demand for nano-TiO_2 currently represents less than 0.6% of TiO_2 pigmentary demand and, for the TiO_2 industry, TiO_2 nanomaterials are considered as niche specialties [22].

Market revenues for titanium dioxide nanopowders in 2009 were estimated around US$ 360 million, and are expected to rise to US$ 1465 million by 2017 [23]. Manufac-turing of nanoscale materials increases the value and, according to company inquiries, nano-TiO_2 is sold between US$ 60 and 180 per kg [24, 25].

3. PHOTOCATALYTIC WATER SPLITTING

3.1. Fundamental Principles

Since the discovery of Fujishima [8], TiO_2 appears as one of the most promising candidates for the fabrication of a commercial photoelectrochemical cell for the production of hydrogen from water [26]. When TiO_2 is irradiated with photons whose energy matches or exceeds the band gap energy of TiO_2, electron-hole pairs are generated. These electron-hole pairs then migrate to the surface, causing redox reactions with the chemical species (electron donors or acceptors) adsorbed on the TiO_2 surface. In particular, in an electrolyte aqueous solution, water molecules are reduced by electrons to form H_2 at the cathode (platinum in Fujishima's experiment) and oxidized by holes to form O_2 at the TiO_2 photoanode [5-6, 8]. Unlike steam reforming, photocatalytic water splitting is an environmentally safe process to generate hydrogen with no greenhouse gas emission (Fig. **1**).
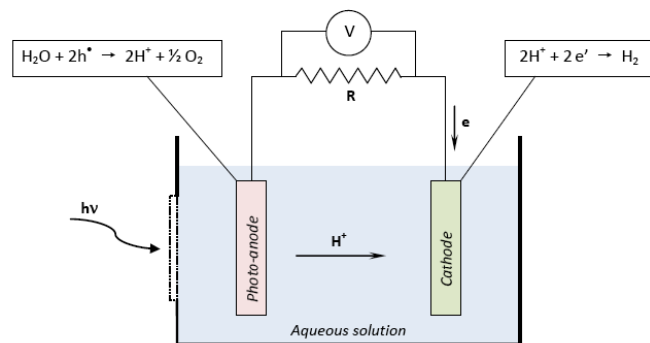

Fig. (1). Schematic principle of a photoelectrochemical cell for photocatalytic water splitting. Cf. text for details. Adapted from [26].

The use of nanoparticles increases the surface area and enhances the concentration of available surface-active sites, thus leading to higher photocatalytic activity. However, an increase in the surface area increases the number of surface defects which are electron-hole recombination centers. Therefore, an optimization of the crystallinity and of the particle size is required to maximize the efficiency of the photoelectrochemical cell [5, 27]. To this end, a large variety of morphologies of TiO_2 nanostructures, including nanoparticles, nanorods, nanowires, nanotubes, mesoporous structures, have been tested as well as diverse synthesis methods [5, 27].

3.2. Challenges for Commercialization

Thirty years after the promising discovery of Fujishima and despite the large amount of research, difficulties in increasing the energy conversion efficiency of photoelectrochemical cells based on nano-TiO_2 above 1% still persist.

According to a report published by the Global Climate and Energy Project of the Stanford University (USA) [28], the efficiency limit of a photoelectrochemical cell is 41% when the band gap of the photoanode exactly matches the

free energy of the water splitting reaction (1.23 eV). The efficiency decreases to about 18% for a band gap of 2 eV and to about 0.05% for a band gap of 3 eV, like in the case of TiO_2.

The critical challenge is therefore to engineer a suitable band gap for maximizing the solar energy absorption by the photoanode semiconductor material. Ongoing research is active to reduce TiO_2 band gap by doping with different ions such as W, Ta, Mo, Cr, etc [26 and refs within] or to extend the absorption region by introducing nitrogen [29]. Carbon was also introduced in TiO_2 and an excellent conversion efficiency of 8.5% was obtained [30]. These results which unfortunately could not be reproduced [26] were however just below the benchmark conversion efficiency of 10% set by the US Department of Energy for commercialization [31, 32]. An overall conversion efficiency of 6.8% has been reported for a photoelectrochemical cell based on TiO_2 nanotubes whose wall thickness was carefully controlled [33].

The resistance of the photoanode material to corrosion by water has to be taken into account as well as the overall lifetime of the system for obvious cost reasons. Besides, for high efficiency of the photoelectrochemical cell, it is not sufficient to reduce the band gap of the photocatalyst. Indeed, minimization of energy losses due to charge recombination and to charge transfer may be achieved through a high crystallinity. A high crystallinity will indeed facilitate the migration of electron-hole pairs to the surface while reducing the defect disorder. Several different nanostructures, such as ordered nanotube arrays, have also been tested to improve the charge transport properties [33, 34]. Moreover, a large surface area, with an increased number of active sites, will enhance the redox reactions taking place at the surface [27]. It is obvious that the control of both microstructure of the photocatalyst and defect structure of its surface layer is a critical point for the optimization of the photoelectrochemical cell [26]. Surface science and surface chemistry also play a key role in determining the active sites on the photocatalysts surface, in controlling the surface defects and in understanding the fundamental mechanisms of band gap engineering. Details on the latest developments of photoelectrochemical cells for solar water splitting and on new promising materials can be found in the January 2011 issue of the MRS Bulletin [35].

As of today, commercialization of the photoelectrochemical water splitting systems is still to become a reality even though companies have been founded. For example, Hydrogen Solar (UK) (http://www.hydrogensolar.com/), founded in 2003, is claiming a "break-through technology for producing high purity hydrogen at competitive commercial rates" but so far no product is for sale.

4. DYE-SENSITIZED SOLAR CELLS (DSSCs)

4.1. Background

The history of the sensitization of large band gap semiconductors for visible light absorption is related in several references (such as [36, 37]). The first demonstration of the conversion of light into electricity in a sensitization solar cell was reported in 1972 [38]. The model system consisted in ZnO (as large band gap semiconductor) sensitized with chlorophyll. The research was active during the following decade

and the achieved energy conversion efficiencies were in the order of 1 to 2.5%. However, stability problems of the organic sensitizers discouraged many research groups to pursue their work in this area.

A breakthrough in the efficiency was reported in 1991 [20]. Based on a film of nanostructured TiO_2 sensitized with a ruthenium complex and on an organic electrolyte, the authors achieved an energy conversion efficiency between 7.1 and 7.9% under simulated solar light illumination. Among others, two factors were responsible for this significant progress: the use of nanostructured TiO_2, providing a large surface area and thus allowing a larger amount of dye molecules to be attached to the TiO_2 surface, and the strong attachment of the dye through the carboxylic groups of the ruthenium complex. The good stability reported by the authors has later been questioned [36] (cf. section 5.2).

Since then, many research groups have been working on improving the performance of DSSCs in terms of either higher energy conversion efficiency or greater stability, and seldom on both simultaneously. To date, the maximum energy conversion efficiency which has been achieved on a cell is 11.1% while the stability of this cell has not been investigated. This record was obtained in the research laboratories of Sharp Corporation (Japan) [39]. A higher efficiency has been recently achieved with more sophisticated devices combining two types of DSSCs (tandem cells) [40].

4.2. Fundamental Principles

DSSCs are based on dye-sensitization of a wide band gap semiconductor [37, 41]. A DSSC is composed of a porous semiconductor (usually TiO_2 or ZnO) covered with an organo-metallic dye (usually a ruthenium complex, such as *cis*-$RuL_2(NCS)_2$, with L=2,2'-bipyridyl-4,4'-dicarboxylic acid, known as N3 dye) immersed in an electrolyte containing a redox couple (usually the I^-/I_3^- system). The semiconductor in contact with a transparent conducting electrode serves as anode, while the cathode (counter electrode) is generally made of platinum or carbon (Fig. **2**).
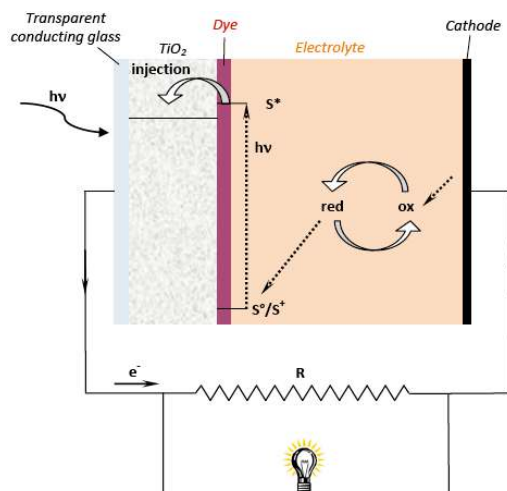

Fig. (2). Schematic principle of a dye-sensitized solar cell: The photoexcitation of the dye (sensitizer, S) generates electrons which are injected into the conduction band of TiO_2. The oxidized dye is regenerated by the electrolyte. Cf. text for details. Adapted from [45].

Unlike in the traditional silicon-based solar cells, in DSSCs the light absorption and the charge separation functions are separated [20]. Under light illumination, the dye molecules interact with the photons and are excited to a state that lies energetically above the conduction band edge of the semiconductor. The photoexcitation of the dye generates electron-hole pairs. While electrons are injected into the conduction band of the semiconductor, holes are left behind in the dye (oxidized state) which is rapidly regenerated (reduced) by the electrolyte, thus preventing back transfer of electrons. Electrons travel through the semiconductor to the transparent electrode and the external load to finally reach the counter electrode where they regenerate the electrolyte [20, 42-45].

Charge separation occurs at the surfaces between the dye, semiconductor and electrolyte. The dye cation is regenerated by the electrolyte before it can recapture the photoelectron. The regeneration of the dye is indeed faster than the recombination reaction of the electron-hole pairs which occurs within a hundred of nanoseconds. Meanwhile, electron injection onto TiO$_2$ conduction band can occur on a fast or ultrafast time scale of the order of picoseconds or hundreds of femtoseconds [42, 45-47].

DSSCs have the great advantage of a very simple fabrication process as proved by the commercial success of educational kits sold by several companies. Kids at high school are able to fabricate their own DSSC with limited and cheap equipment.

4.3. Cost Model

The position of every solar device on the market is determined by three factors: efficiency, lifetime and cost [48]. According to Brabec [48], commercialization can be fully successful only if these three requirements are fulfilled at the same time with an optimum balance: (i) reasonable energy conversion efficiency, (ii) optimized lifetime of the device, and (iii) competitive costs. If only two out of these 3 factors are acceptable, the product may only address niche markets. It is believed that low-cost solar cell technologies will be acceptable from a commercial point of view if cells show efficiencies at least between 5 and 10% and lifetime between 5 and 10 years [49]. The final cost of the power generation will also depend on module and installation costs for the application.

As of to date, the best DSSCs built in laboratory exhibit a power conversion efficiency around 11%, with corresponding module efficiencies ranging from 3 to 5% [50].

The low cost of the DSSC fabrication process is not a subject of controversy, although, to the author's best knowledge, no exact cost calculation has been published for a solar cell based on dye-sensitized nanostructured TiO$_2$. The cost of a cell actually depends on the dye and on the TiO$_2$ synthesis and deposition processes which are adopted for the device fabrication. However, according to Samsung SDI, the manufacture cost of DSSC would be around 1/3 to 1/5 the cost of existing semiconductor solar cell [51]. But it has to be underlined that the important R&D efforts deployed to increase the energy conversion efficiency of DSSCs may add to the complexity of the system and may drastically increase the

cost of the cell, and therefore will not necessarily increase the chances for successful commercialization. Obviously, a basic necessary condition for the device to be viable is that, during its lifetime, it produces more energy than it is necessary to produce and recycle it.

The most critical parameter in the achievement of marketable DSSCs appears to be the stability over extended periods of time. Whereas the stability of silicon-based solar modules is not questioned for a lifetime of 10 to 20 years, the dye and the electrolyte in DSSCs have to be stable enough to reversibly undergo millions of oxidation and reduction cycles [52]. Extensive studies have been performed by different research groups and results are strongly divergent [36, 37, 45, 52-55] (cf. section 5.2).

4.4. Commercialization

According to a report published by the business research and consulting company Frost & Sullivan [56], "*the exploratory mass production of DSSC-powered consumer durables is likely to alter the future course of research*" in the field of third generation photovoltaics. The 4th international conference on the industrialization of dye solar cells (DSC-IC 2010) was held in Colorado Springs (CO, USA) on 1-4 November 2010, giving the latest developments of DSSC components, summarizing the best performances achieved worldwide with an overview of the industrialization perspectives [57].

As of to date, large companies (particularly in Asia) involved in the solar energy business definitely show an interest in this promising technology and have an R&D activity on DSSCs (e.g. Sharp, Samsung, Sony, Fujikura), but do not yet commercialize any product. Smaller companies or recently founded start-ups are tentatively introducing products on the market. The main applications of DSSCs are likely to be in consumer electronics and wireless technologies, at least as a first step to the market.

Here are some examples of those companies:

- **Solaronix** (Switzerland): The company produces components for the development and the fabrication of DSSCs. It commercializes demonstration DSSCs and their electric accessories, interconnected DSSC modules (up to 30x30 cm and 11 cells), and equipment for evaluation and ageing of solar cells. But, for the interconnected DSSC modules, the company website clearly mentions "*This solar module is not an industrial product but a prototype*" (http://www.sola-ronix.com)

- **3GSolar** (Israel): 3GSolar is developing DSSC modules in collaboration with Solaronix. But, quoting the company website: "*Please note 3GSolar does not yet produce solar modules*" (http://www.3gsolar.com)

- **G24 Innovations** (UK/USA): One product is for sale which consists in a solar charger made of a DSSC panel associated with a nickel-hydride battery (http://www.g24i.com)

- **SolarPrint** (Ireland): SolarPrint is developing a high volume manufacturing line for DSSC but does not yet produce any module (http://www.solarprint.ie)

- **Dyesol** (Australia): Dyesol is mainly a supplier of equipment, materials and components for DSSC fabrication (dyes, powders, pastes,). The company does not sell any module but educational kits (http://www.dyesol.com)

- **Timo Technology** (Korea) has signed a joint venture agreement with Dyesol in 2007 and is building a pilot line for DSSC manufacturing (http://www.timo.co.kr)

- **Sol Ideas** (USA) is a consulting firm in the field of optics and semiconductors for optoelectronics, photovoltaics and renewable energy, and is selling DSSC educational kits (http://www.solideas.com)

- **Sharp Solar** (Japan): In Sharp Solar laboratory, the best power conversion efficiency has been achieved but DSSCs are not commercialized by the company (http://sharp-solar.com)

- **Everlight Chemical Industrial Corporation** (Taiwan): For sale, are only components involved in the development and the fabrication of DSSCs (dyes, TiO_2 pastes, etc) (http://www.ecic.com)

- **Konarka** (USA): Even if Konarka has been granted licensee rights to develop dye-sensitized solar cell technology in 2002, no product appears to be for sale yet (http://www.konarka.com).

5. TOWARD IMPROVED DSSCs

During the last 10 years, research has been actively going on to improve the performance of DSSCs, addressing each component of the cell: (i) the semiconductor material (photoanode) which is the electron transporting layer, (ii) the dye (photosensitizer), (iii) the electrolyte (electron transfer mediator) and (iv) the counter-electrode (catalyst of the electron transfer) [45, 58]. Optimized fabrication procedures and understanding of the charge transport mechanisms are also key factors in this improvement process.

Focusing only on the use of TiO_2 for solar cells, the number of papers published in this field can be considered as a rough indicator of the exploding growth of the research activities on DSSCs during these last 10 years. A rapid literature search in the "*Current Contents*" database (*ISI Web of Knowledge of Thomson Reuters*) [59] with the keywords "*TiO_2*" and "*solar cells*" shows that the number of published papers increased from 75 in 2000 to 1045 in 2010 (Fig. **3**).

In terms of patents, a search on the World Intellectual Property Organization (WIPO) Search Service website [60] with the keyword "*dye sensitized solar cell*" in the full text of the patent shows that 1042 patents were published between 2000 and 2010, about half of them being published internationally under the Patent Cooperation Treaty (PCT) and about 30% of them published under the European Patent Office (EPO). A search with the keywords "*dye sensitized solar cell*" and "*oxide*" in the full text gives 741 patents published between 2000 and 2010, whereas a search with the keywords "*dye sensitized solar cell*" and "*TiO_2*" results in 367 patents published during the same 10-year period. Fig. (**4**) gives the distribution of the published patents per year from 2000 to 2010 for the two searches: the first one with the
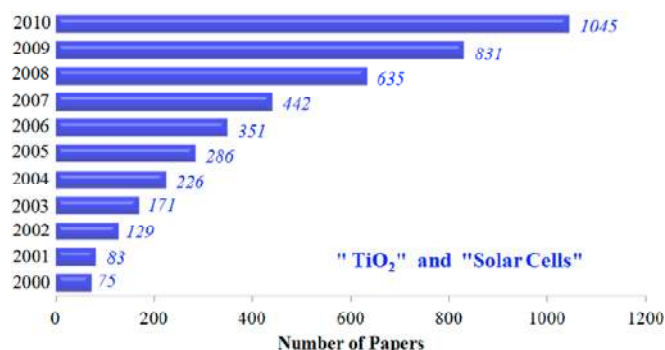

Fig. (3). Number of papers published per year (from a literature search in the *Current Content* database with the keywords "TiO_2" and "Solar cells").
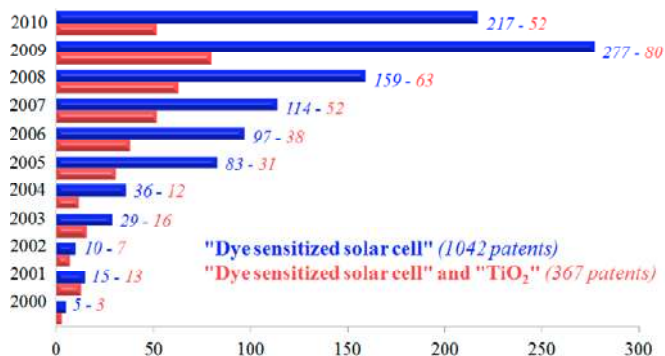

Fig. (4). Number of patents published per year (from searches on the WIPO website with the keyword "Dye-sensitized solar cell" and with the keywords "Dye-sensitized solar cell" and "TiO_2").

keyword "*dye sensitized solar cell*" and the second one with the keywords "*dye sensitized solar cell*" and "*TiO_2*".

Obviously, it is out of the scope of this paper to review all these results. Only some points are outlined below with an emphasis on TiO_2.

5.1. Improved Fabrication, New Components, New Approaches

Semiconductor electrode: TiO_2 is definitely the preferred semiconductor material with ZnO as an alternative [27, 47, 61]. The efficiency of the cell is strongly dependent of the quality of the semiconductor film. Absence of cracks and defects together with a good crystallinity are needed for an efficient electron flow [62-65]. In addition, a large surface area is required to allow a maximum adsorption of the dye while an intimate contact between the semiconductor surface and the dye should be ensured for maximum efficiency [46, 66, 67]. The mesoporous structure appears to be of particular interest increasing the interactions of the semiconductor with the electrolyte [5, 37, 68, 69].

Different electrode nanostructures have been tested such as nanoparticles, nanotubes, nanowires, or nanorods [5, 58, 62, 70-72]. Ordered arrays of nanotubes, nanowires or nanorods as well as mesoporous structures have been proved to increase the energy conversion efficiency of DSSCs [17, 40, 69-71, 73-75].

Anatase is usually the preferred crystalline phase because the electron transport has been demonstrated to be faster than in the rutile phase [7, 17, 73, 76]. But mixtures of anatase and rutile have also been investigated [77]. Studies have additionally been reported on doping TiO_2 with different elements, such as nitrogen [78], and on TiO_2-based composite structures containing C_{60} [79] or carbon nanotubes [80].

Sensitizer (dye): A development direction toward an improved dye consists in the enhancement of its photoresponse in the near IR region by engineering its molecular structure [37, 81]. Dyes have to fulfill several requirements like absorption in the visible region, efficient electron injection to the conduction band of the semiconductor, high stability, and reversibility of their redox chemistry [81, 82]. Obviously, the dye molecule should bear suitable anchoring groups to strongly attach to the TiO_2 surface [66, 81] while forming a monolayer to maximize the injection of the photoelectrons in the semiconductor. Indeed, the efficiency of the DSSC is strongly influenced by the thickness, the morphology and the homogeneity of the dye layer [43] and it has been proved that aggregates, even as small as dimers, dramatically reduce the photocurrent efficiency [83]. Therefore, the anchoring groups play an important role not only in the overall performance of the cell but also in its long-term stability [84]. The carboxyl group is generally regarded as one of the most efficient chemical groups to provide a stable attachment to the TiO_2 surface [66, 68, 84-87]. New dyes, often based on ruthenium complexes as well as on alternatives, are continuously investigated [81, 84, 86, 88, 89]. Tuning the electronic interactions between the dye and the TiO_2 surface is also envisaged by designing "supramolecular" compounds [68 and refs within].

Electrolyte: Amongst the many problems compromising the long-term stability of the DSSC performance, the leakage of the liquid electrolyte is one of the critical factors currently preventing DSSCs from successful commercialization on a large scale. Besides improved sealing of the cell, solid or quasi-solid (gels) electrolytes are being proposed as alternatives to the popular I^-/I_3^- system [90].

Quantum dots sensitized solar cells (QDSSCs): Recently, a new approach to DSSCs consists in replacing the organo-metallic dye by short band gap semiconductor quantum dots (QDs), such as InP, InAs, CdSe, CdS or PbS [91-98]. In the QDSSCs, the quantum dots serve as sensitizers and electrons are transferred to the TiO_2 wide band gap semiconductor. The size quantization property allows one to tune the visible response and by varying the size of the QDs, the QDSSCs can be tuned to absorb particular wavelengths ("rainbow solar cells") [69, 92, 99]. In some cases, organic linkers are used to attach the QDs to the TiO_2 surface [92] while in other cases, in situ QD deposition is performed *via* their precursor solutions (SILAR process) [96, 98]. Reported power conversion efficiencies of QDSSCs are not yet competitive with those of regular DSSCs [93].

5.2. Stability and Degradation Mechanisms

The performances of the DSSCs are currently limited by many factors, including degradation of the dye, leakage of

the electrolyte, corrosion of the counter-electrode, poor quality and morphology of the semiconductor film leading to fast recombination of electron-hole pairs [71]. The poor long-term stability seems to be the most critical feature which has prevented DSSCs from a commercial success to date. A critical review of the stability studies has been published in 2004 by Figgemeier and Hagfeldt [53] and since then, progress toward detailed understanding of the physics and chemistry of DSSCs has remained slow due to the complexity of the system. This section outlines only a few of the major points carefully reported and analyzed in Figgemeier's article where more details can be found. It has to be noted that the results of the different stability studies published so far are extremely dependent on the cell fabrication parameters and on the measurement conditions.

Most attention is paid to the stability of the dye during DSSC operation as it is a subject of controversy. Whereas in some studies, the N3 dye can sustain 10^8 redox cycles (corresponding to 20 years of continuous operation) without noticeable loss of performance [100], in other studies the lifetime of the cell is so poor that stability measurements could not even be performed [36]. It has been reported that the dye in its oxidized state degrades through the loss of sulfur and therefore the rapid regeneration of the dye is one of the requirements for ensuring the cell stability [37]. A possible reason for the dye instability observed in some cells could be an insufficient iodide concentration in the electrolyte, thus limiting the regeneration of the dye [45, 52]. Using photocurrent imaging techniques, it appeared that the kinetics of the degradation of the cells is not homogeneous and that a key factor could be the concentration of the sensitizer buffering the degradation process in some areas of the cell. It was also noted that the N3 dye quickly degrades when exposed to ambient air, oxygen or humidity [64, 101], to temperatures higher than 125°C or to UV irradiation [101]. Another key question on the sensitizer degradation is the role played by the surface chemistry of TiO_2 [55] which at this point has not been elucidated (cf. section 6.2).

Sealing must be efficient so that pollutants, particularly water and oxygen, do not penetrate into the cell as it has been found that the degradation of the electrolyte can be strongly accelerated by the presence of water [53-55]. Poor sealing may also lead to evaporation and thus to the formation of bubbles [54]. In addition, the electrolyte solvent has a significant effect on the stability because any trace of water in the solvent can trigger hydrolysis reactions.

The physical and chemical nature of the TiO_2 surface appears as a crucial parameter to control the stability and the efficiency of the cell. Indeed, the surface charge influences the position of the conduction band edge and the Fermi level. In addition, the surface states (such as Ti^{4+} ions) and the surface reactivity can lead to the decomposition of the electrolyte or the dye [53]. The back electron transfer reaction is very sensitive to the chemical nature of the TiO_2 surface [46] and the binding geometry of the dye molecules adsorbed onto the TiO_2 surface is determined by the TiO_2 surface chemistry [46] (cf. section 6.5). In turn, the binding geometry of the dye may influence the electron injection into the

semiconductor [42-43]. It also has to be noted that possible diffusion of platinum from the counter electrode can affect TiO_2 electrical and catalytic properties [53].

In any case, as pointed out by Figgemeier and Hagfeldt [53], accelerated testing of DSSC to simulate cell ageing over a 10-year period, remains a challenge because the parameters used for the accelerated testing do not necessarily reflect the long-term working conditions (e.g. higher light intensity). Therefore, fundamental understanding of the interactions between the DSSC components and of all physical and chemical phenomena taking place in a DSSC under operation is an absolute requirement to achieve stable and commercially viable cells.

6. OUR CONTRIBUTION TO THE IMPROVEMENT OF DSSCs: INFLUENCE OF THE TiO_2 SURFACE CHEMISTRY ON THE DYE ATTACHMENT

6.1. Complexity of DSSCs in terms of Surfaces and Interfaces

The simplicity and cost-effectiveness of the standard fabrication process, leading to basic DSSCs like those proposed in educational kits, should not hide the complexity of the whole system. Indeed, in terms of interfaces and surface chemistry, DSSCs constitute extremely complex systems. Excluding the two electrodes, the core of the photoelectrochemical system includes several components which are not always precisely described in the many articles. Moreover, the origin of these components varies, which may lead to variations in the interfaces composition and therefore to differences in the interactions between the components.

- Firstly, the TiO_2 material may be a commercial product, or prepared in the lab according to different synthesis methods. Obviously, synthesis parameters vary from a research team to the other, leading to different particle shape and size, crystallinity, and surface chemistry.

- Secondly, depending on the origin of the TiO_2 particles, a solvent or a solvent mixture (sometimes including a surfactant) is used to obtain a colloid or a paste which is applied on the transparent electrode. Then, the TiO_2 film is dried and generally fired at 450°C in air.

- Thirdly, the dye based on ruthenium (such as N3, N719, N712) is dissolved in a solvent or a solvent mixture. The fired TiO_2 film is dipped, generally still warm, in the dye solution.

- Finally, a solution containing the iodine-based electrolyte fills the cell.

Moreover, various additives are sometimes used to improve efficiency or stability of the cell. So, as already noted [53], it is extremely difficult to establish sound comparison between the results published by different research groups.

6.2. Surfaces and Interfaces in DSSC Performance

Interfaces and surface chemistry of the TiO_2 nanostructure play critical roles in the functioning of DSSCs [43] and eventually impact the energy conversion efficiency and the stability of the final device. However, these aspects are not always taken into consideration in the many research works.

Fig. (**5**) shows the number of papers published between 2000 and 2010 as obtained from a rapid literature search in the "*Current Contents*" database [59] with different combinations of keywords ("*TiO_2*", "*solar cells*", "*interface*", "*surface*", "*surface chemistry*"). One can roughly conclude that 35% of the papers including the keywords "*TiO_2*" and "*solar cells*" also include the keyword "*surface*" whereas 10% include "*interface*" and only 0.3% "*surface chemistry*". Obviously, Fig. (**5**) does not give an exact picture of the research efforts deployed worldwide on DSSCs, but the general trend indicates that the surface chemistry of the TiO_2 nanostructure has not yet been clearly identified by most researchers as a critical factor to be investigated and systematically controlled for DSSC optimization.
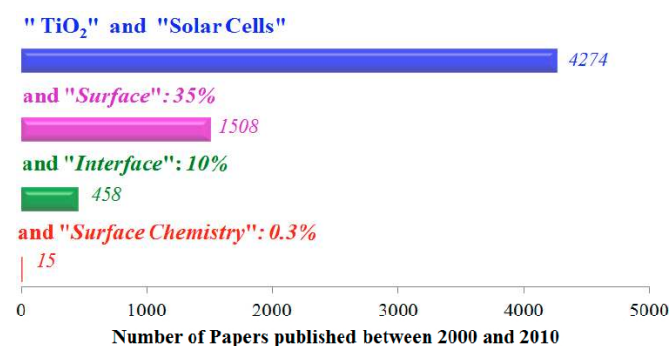

Fig. (5). Number of papers published between 2000 and 2010 (from a literature search in the *Current Content* database with different combinations of keywords).

Nevertheless, several research groups point out that the structure and the chemistry of the TiO_2 surface affect the binding geometry for the adsorbed dye molecules while, in turn, the type of the binding and the geometry of the bound dye molecules influence the efficiency of the charge injection from the dye to TiO_2 and possibly the overall stability of the cell [26, 46, 84-87]. Experiments show that the rate of the interfacial electron transfer can be very sensitive to small changes in the preparation of the semiconductor sample, the state of the surface and the proton concentration [46, 85]. Therefore, the efficiency of the cell is dependent on the surface properties of TiO_2 [62] and, as a consequence, the determination of the appropriate conditions for dye anchoring through surface treatment and/or tailoring of the TiO_2 nanoparticles is an important parameter for final optimization of DSSCs [87].

6.3. Fourier Transform Infrared (FTIR) Spectroscopy for the Study of DSSCs

To study the attachment of the dye molecules to the TiO_2 surface, Fourier transform infrared (FTIR) spectroscopy is one of the preferred techniques. FTIR spectroscopy is indeed a powerful tool to investigate the adsorption of organic molecules on nanoparticle surfaces, to monitor the surface reactions, to probe the surface reactive sites and to characterize the chemical species eventually attached to the nanoparticle surface [102-103]. This technique has been used by several research groups to study the binding of the dye molecule to the TiO_2 surface [36, 66, 68, 87, 88, 101]. However, in most cases, the dye-sensitized solar cell is studied as a
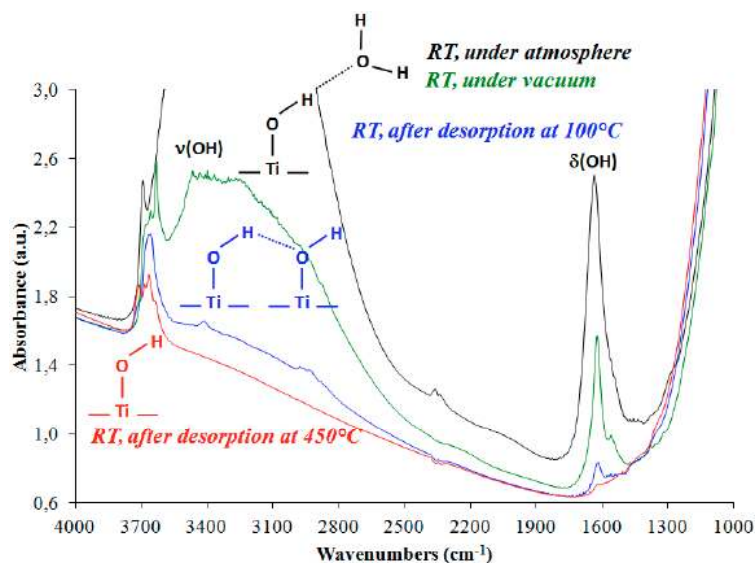
Fig. (6). FTIR surface spectrum of TiO₂ nanoparticles at room temperature: (black) under atmosphere; (green) under dynamic vacuum; (blue) after desorption at 100°C; (red) after desorption at 450°C.

whole to directly correlate the IR results with other cell characteristics, such as efficiency or stability. But, the complexity of the system due to the large number of components and additives, all of them absorbing in the infrared range, does not allow a precise investigation of the chemical nature of the dye attachment to TiO₂. In addition, the TiO₂ surface chemistry is seldom investigated prior to the dye attachment even though, as previously mentioned, it definitely has an influence on the binding. In other IR studies, the dye molecule is simulated with smaller molecules in order to get a deeper understanding of the attachment to TiO₂ [109-111]. It is this later approach that we have followed in our study as briefly described below.

It has to be noted that the purpose of this section is to highlight a technique for the analysis of the surface chemistry of the TiO₂ nanoparticles and to emphasize that, depending on the TiO₂ pre-treatment conditions, the dye molecules can attach differently to the TiO₂ surface, which, according to the literature and as explained in sections 5.2 and 6.2, may have consequences on the DSSC efficiency. This section is not intended to thoroughly describe the infrared study of the TiO₂ surface chemistry and to discuss the geometry and stability of the dye attachment to the TiO₂ surface. Another article specifically dedicated to the IR spectroscopic study of the dye attachment to the surface of TiO₂ nanoparticles is currently under preparation.

It is agreed that the carboxylic functional groups of the dye molecule serve as grafting agents to the TiO₂ surface even though the anchoring nature is still under debate as well as the role of the OH groups at the TiO₂ surface [66, 84-88].

Our contribution to the improvement of the DSSC performance is to study the attachment of the carboxylic group to the TiO₂ surface as a function of the preparation or pretreatment conditions of the TiO₂ material, and to elucidate the role played by the OH groups at the TiO₂ surface in the attachment. For this purpose, the acetic acid molecule, which contains one carboxylic group is taken as a case study schematically representing the dye molecule. It is obvious that our experiments do not reflect a real DSSC under its operating conditions but our final objective is the optimization of the DSSC fabrication process through the understanding of surface phenomena on model systems.

The setup for the FTIR analyses has been described elsewhere as well as the sample preparation conditions and the experimental procedure [102, 112, 113]. The experiments were performed *in situ* by FTIR spectroscopy in transmission mode. The TiO₂ nanoparticles used for these studies are a mixture of the anatase (70%) and rutile (30%) phases (P25 from Degussa) and the average primary particle diameter is 21 nm with a specific surface area of 50 ± 15 m²/g. The TiO₂ nanoparticles, slightly pressed into a thin pellet, are desorbed under dynamic vacuum at temperatures chosen to best fit the different steps of the DSSC standard fabrication procedure.

We study the interactions of acetic acid with the TiO₂ surface depending on the TiO₂ pretreatment conditions which lead to different levels of surface hydration and hydroxylation.

6.4. FTIR Surface Spectra of TiO₂ Nanoparticles

The infrared spectrum of the surface of the TiO₂ nanoparticles is shown in Fig. (**6**) as a function of the desorption temperature. The two main absorption regions (3750-2800 cm⁻¹ and 1700-1500 cm⁻¹) are due to the stretching and bonding vibrations of the OH bonds, ν(OH) and δ(OH), both in OH groups directly linked to the TiO₂ surface and in adsorbed water molecules. After evacuation at room temperature, part of the OH groups at the TiO₂ surface is freed from hydrogen-bonded water. After desorption at 100°C, most of the hydrogen-bonded water molecules have been eliminated and the absorption bands are due to surface OH groups either isolated or interacting with other adjacent surface OH groups. After desorption at 450°C, only isolated surface OH groups remain with their absorption frequencies in the 3750-3600 cm⁻¹ region.
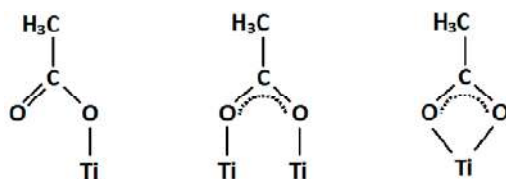
Fig. (7). Possible geometries for carboxylate species coordinated on a metal oxide surface. From left to right: monodentate, bridging bidentate, chelating bidentate.

The multiplicity of the $\nu(OH)$ absorption bands indicates the presence of different types of OH groups at the TiO_2 surface, which is due to the different coordination states of the Ti atoms within the surface and to the different crystalline exposed faces of both rutile and anatase phases [114-121]. Obviously these different OH surface groups have different acido-basicity [114-117]. Hence, the infrared surface spectrum of the TiO_2 nanoparticles desorbed at 450°C gives information on the surface chemistry of the nanoparticles and on its reproducibility over different batches and over different synthesis conditions or methods.

The many studies of the TiO_2 surface chemistry have proved that both acidic and basic sites are present on TiO_2 surfaces [114, 117, 118, 120, 122-124] and that the surface chemistry of TiO_2 is very dependent on the degree of the surface hydration, on the sample preparation conditions and on the presence of impurities [114, 118-120, 124].

6.5. Adsorption of Acetic Acid on TiO_2 Nanoparticles

Besides molecular adsorption, carboxylic acids can strongly coordinate to metal oxide surfaces *via* dissociative adsorption involving the breakage of the OH bond [109, 125-129]. The participation of the OH groups on the metal oxide surface leads to the formation of water. The carboxylate species resulting from the carboxylic acid dissociation may bind to the metal oxide surface according to different geometries, such as monodentate, bridging bidentate or chelating bidentate species (Fig. **7**) depending on the surface chemistry of the metal oxide and on the crystalline structure of the exposed faces [125, 130]. In addition to the thermal stability of

the adsorbed species which gives information on the strength of the binding, it has been demonstrated that the wavenumber separation ($\Delta\nu$) between the asymmetric $\nu_{as}(COO)$ and symmetric $\nu_s(COO)$ CO stretching frequencies (1700-1200 cm^{-1} range) of the attached carboxylate species gives an indication of their binding geometry. For monodentate species, $\Delta\nu$ is much larger than the wavenumber separation for ionic complexes ($\Delta\nu_{ionic}$ around 140 cm^{-1}) whereas for bidentate species, $\Delta\nu$ is much less than $\Delta\nu_{ionic}$. Bridging bidentate species generally exhibit larger $\Delta\nu$ values than chelating bidentate species, close to $\Delta\nu_{ionic}$ [109, 130-135].

The IR spectrum of the adsorption of acetic acid at 100°C on the TiO_2 nanoparticles desorbed at 450°C is presented in Fig. (**8**). As soon as acetic acid is in contact with this pretreated TiO_2 surface, all surface OH groups are completely and immediately eliminated as indicated by the disappearing of the $\nu(OH)$ absorption bands in the 3750-3600 cm^{-1} region. The two strong bands at 1535 and 1452 cm^{-1} are respectively assigned to the $\nu_{as}(COO)$ and $\nu_s(COO)$ vibrations in acetate groups coordinated to the TiO_2 surface. No absorption band above 1700 cm^{-1} which would have been indicative of the presence of C=O bonds is observed. According to the Deacon's rule [134-135], the wavenumber separation between $\nu_{as}(COO)$ and $\nu_s(COO)$ ($\Delta\nu = 83$ cm^{-1}) indicates a coordination in bidentate geometry and suggests a chelating configuration. However, it appears that this type of geometry is unlikely on titania as it would lead to hepta-coordinated Ti^{4+} [109]. Density functional calculations together with photoelectron diffraction, STM and AFM studies also argue in favor of a bridging bidentate geometry [125, 136, 137]. As expected, these bridged acetate species are quite stable. They indeed resist a desorption at 300°C and they are mainly eliminated at 450°C.

As explained above, when TiO_2 is desorbed at 100°C only, the surface OH groups are not yet totally isolated from each other (spectra not shown). In this case also, acetic acid adsorption leads to the formation of acetate groups. However, even after a 30-minute contact, the $\nu(OH)$ absorption band (centered at 3654 cm^{-1}) of the OH groups at the TiO_2 surface is still clearly visible indicating that only part of
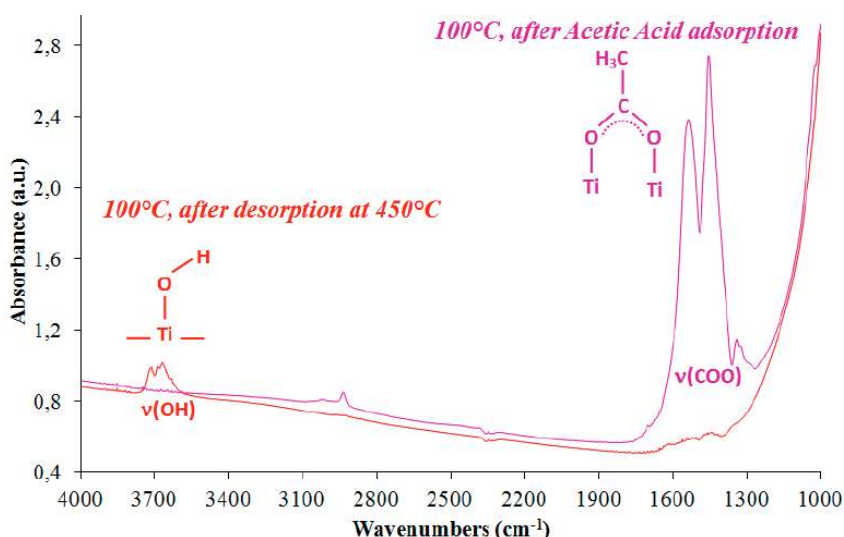

Fig. (8). FTIR surface spectrum of TiO_2 nanoparticles at 100°C: (red) after desorption at 450°C; (pink) after adsorption of acetic acid at 100°C.
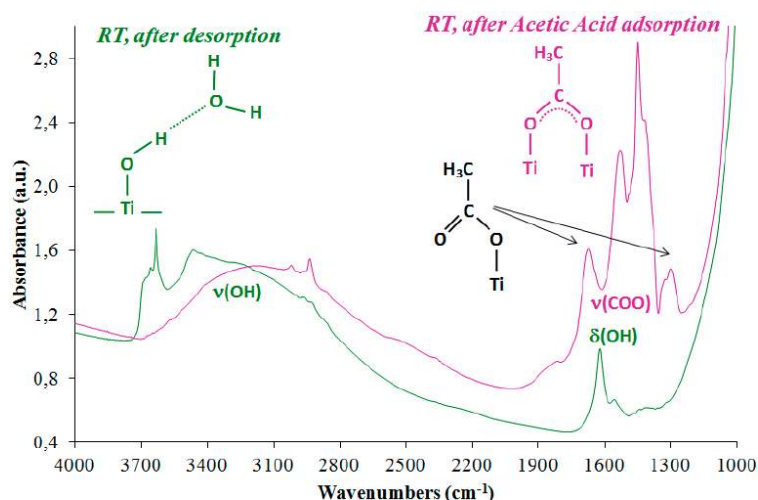
Fig. (9). FTIR surface spectrum of TiO$_2$ nanoparticles at room temperture: (green) under dynamic vacuum; (pink) after adsorption of acetic acid at room temperature.

these surface OH groups participate in the attachment. The shapes and frequencies of the ν_{as} (COO) and ν_s(COO) absorption bands (1530 and 1451 cm^{-1} respectively) of the attached acetate species are similar to those observed on the TiO$_2$ surface pre-treated at 450°C. Like in the previous case, these bridging bidentate acetates are mainly eliminated by desorption at 450°C.

When TiO$_2$ is only desorbed at room temperature, a large part of the OH groups at the TiO$_2$ surface is hydrogen-bonded (cf. Fig. **6**). When acetic acid is adsorbed at room temperature on such TiO$_2$ surface (Fig. **9**), the frequency shift of the broad band centered at 3270 cm^{-1} to 3190 cm^{-1} together with the decrease of the OH bending band at 1622 cm^{-1} prove that hydrogen-bonded water molecules are released and replaced with acetic acid molecules which form new hydrogen bonds with the surface OH groups. Indeed, acetic acid interacts more strongly with the TiO$_2$ surface than water and can displace water molecules from the surface [125, 138]. Acetate species are then steadily formed and, like in the previous two cases, adsorbed on the surface in the bridging bidentate geometry (absorption bands at 1529 and 1449 cm^{-1}). Also similarly to the previous two cases, the surface OH groups which are not hydrogen-bonded are consumed in the adsorption of acetic acid as proved by the disappearing of their corresponding absorption bands in the 3650 cm^{-1} region.

Besides, two new bands are observed in the ν(COO) absorption range at 1672 and 1301 cm^{-1}. The wavenumber separation is about 370 cm^{-1} and, according to the Deacon's rule, this $\Delta\nu$ value indicates the formation of monodentate acetate species. A desorption at 100°C eliminates hydrogen bonded species while the two bands at 1672 and 1301 cm^{-1} disappear. This disappearing that could be correlated with the increase of the 1529 and 1449 cm^{-1} bands would be explained by the transformation of monodentate acetates into bridging bidentate acetates. This would be consistent with the results of DFT calculations on formic acid adsorption on anatase which suggest that even though bridging bidentate species are more stable that monodentates, an energy barrier needs to be overcome for monodentate to transform into bridging bidentate [125, 131].

In summary, whatever the pretreatment of the TiO$_2$ nanoparticles, acetic acid strongly coordinates to the TiO$_2$ surface as acetate species preferably in the bridging bidentate geometry. In parallel, OH groups are removed from the TiO$_2$ surface, thus indicating their involvement in the coordination of acetic acid molecules and the formation of water.

When the TiO$_2$ sample is simply desorbed at room temperature, water molecules hydrogen-bonded to the TiO$_2$ surface are released and replaced with acetic acid molecules. Simultaneously, acetate species are formed which coordinate in both monodentate and bridging bidentate geometries. The former species transform into the more stable bridging bidentate acetates by heating at 100°C. In this case also, OH groups not involved in hydrogen bonds participate in the coordination of acetic acid molecules and are removed from the TiO$_2$ surface.

From these experiments it can be concluded that the TiO$_2$ nanoparticles should undergo a heat treatment to 450°C before dye adsorption in order to minimize the presence of water and maximize the strength of the dye attachment.

As the TiO$_2$ pastes used for the DSSC fabrication are often based on alcoholic media, we have also studied the interactions of acetic acid with the TiO$_2$ surface on which ethanol has been initially adsorbed. It is indeed known that ethanol can strongly react with metal oxide surfaces [110-111] and that alcohols and carboxylic acids can compete to adsorb on such surfaces [138]. Our latest results are being submitted for publication.

CONCLUSIONS AND PERSPECTIVES

Independently of its large use as white powder pigment, titania exhibits multiple properties which make this material particularly attractive for various high-added value applications, particularly those related to medicine and environment protection. In the field of clean energy, photocatalytic water splitting and dye-sensitized solar cells definitely benefit from titania processed at the nanometer scale. However, after 20 years of research at least, these two applications have not yet found their way to successful commercialization. Many problems are still to be solved, specially at the surfaces and

interfaces in systems as complex as DSSCs. Amongst the major challenges to be taken up, the surface chemistry of nano-titania certainly represents a critical parameter to be controlled, mastered and monitored for reproducible and sustainable improvement of DSSCs.

CONFLICT OF INTEREST

None Declared.

ACKNOWLEDGEMENT

None Declared.

REFERENCES

[1]   Reck, E.; Richards, M. Titanium dioxide — Manufacture, environment and life cycle analysis: The tioxide experience. *Surf. Coat. Int., Part B: Coat. Trans.*, **1977**, *80*, 568-572.

[2]   Wang, Z.; Helmersson, U.; Käll, P.-O. Optical properties of anatase TiO$_2$ thin films prepared by aqueous sol–gel process at low temperature. *Thin Solid Films*, **2002**, *405*, 50-54.

[3]   ICIS Chemical Industry News website: http://www.ic-is.com/v2/chemicals/9076546/titanium-dioxide/uses.html (accessed: June 27, 2011).

[4]   Ertl, G.; Knözinger, H.; Schüth, F.; Weitkamp, J. (Eds.). *Handbook of Heterogeneous Catalysis*; Wiley-VCH Verlag GmbH& Co. KGaA: Weinheim (Germany), **2008**, Vol. 4.

[5]   Chen, X.; Mao, S.S. Titanium dioxide nanomaterials: Synthesis, properties, modifications and applications. *Chem. Rev.*, **2007**, *107*, 2891-2959.

[6]   Linsebigler, A.L.; Lu, G.; Yates Jr., J.T. Photocatalysis on TiO$_2$ surfaces: Principles, mechanisms, and selected results. *Chem. Rev.*, **1995**, *95*, 735-758.

[7]   Wold, A. Photocatalytic properties of TiO$_2$. *Chem. Mater.*, **1993**, *5*, 280-283.

[8]   Fujishima, A.; Honda, K. Electrochemical photolysis of water at a semiconductor electrode. *Nature*, **1972**, *238*, 37-38.

[9]   Gu, Z.-Z.; Fujishima, A.; Sato, O. Patterning of a colloidal crystal film on a modified hydrophilic and hydrophobic surface. *Angew. Chem. Int. Ed.*, **2002**, *41*, 2067-2070.

[10]   Sirghi, L.; Hatanaka, Y. Hydrophilicity of amorphous TiO$_2$ ultra-thin films. *Surf. Sci.*, **2003**, *530*, L323-L327.

[11]   Nordic Mining website: http://www.nordicmining.com/ and http://www.engeboprosjektet.no/ (accessed: June 27, 2011)

[12]   Artikol website: http://www.artikol.com (accessed: June 27, 2011)

[13]   Tian, G.-L.; He, H.-B.; Shao, J.-D. Effects of microstructure of TiO$_2$ thin films on optical band gap energy. *Chin. Phys. Lett.*, **2005**, *22*, 1787-1789.

[14]   Wunderlich, W.; Miao, L.; Tanemura, M.; Tanemura, S.; Jin, P.; Kaneko, K.; Terai, A.; Nabatova-Gabin, N.; Belkada, R. Ab-initio calculations of the optical band-gap of TiO$_2$ thin films. *Int. J. Nanosci.*, **2004**, *3*, 439-445.

[15]   Zhang, H.; Banfield, J.F. Thermodynamic analysis of phase stability of nanocrystalline titania. *J. Mater. Chem.*, **1998**, *8*, 2073-2076.

[16]   Berger, T.; Sterrer, M.; Diwald, O.; Knözinger, E.; Panayotov, D.; Thompson, T.L.; Yates Jr., J.T. Light-induced charge separation in anatase TiO$_2$ particles. *J. Phys. Chem. B*, **2005**, *109*, 6061-6068.

[17]   Pavasupree, S.; Jitputti, J.; Ngamsinlapasathian, S.; Yoshikawa, S. Hydrothermal synthesis, characterization, photocatalytic activity and dye-sensitized solar cell performance of mesoporous anatase TiO$_2$ nanopowders. *Mater. Res. Bull.*, **2008**, *43*, 149-157.

[18]   Cai, R.; Hashimoto, K.; Kubota, Y.; Fujishima, A. Increment of photocatalytic killing of cancer cells using TiO$_2$ with the aid of superoxide dismutase. *Chem. Lett.*, **1992**, 427-430.

[19]   Sunada, K.; Watanabe, T.; Hashimoto, K. Studies on photokilling of bacteria on TiO$_2$ thin film. *J. Photochem. Photobiol. A*, **2003**, *156*, 227-233.

[20]   O'Regan, B.; Grätzel, M. A low-cost, high-efficiency solar cell based on dye-sensitized colloidal TiO$_2$ films. *Nature*, **1991**, *353*, 737-740.

[21]   Nanoposts Report: *Commercial applications for photocatalytic nanoparticle titania*, published Oct. 2010: http://www.nanoposts.moonfruit.com/ (accessed: June 27, 2011).

[22]   DuPont Report: *Titanium dioxide: A brief overview of TiO$_2$ pigments compared with TiO$_2$ nanomaterials*, Mars 2010: http://www.dtsc.ca.gov/TechnologyDevelopment/Nanotechnology/upload/Whiting-_TiO2_Uses.pdf (accessed: June 27, 2011).

[23]   MarketResearch website: http://www.marketresearch.com/ (accessed: June 27, 2011).

[24]   Ogilvie Robichaud, C.; Uyar, A.E.; Darby, M.R.; Zucker, L.G.; Wiesner, M.R. Estimates of upper bounds and trends in nano-TiO$_2$ production as a basis for exposure assessment. *Environ. Sci. Technol.*, **2009**, *43*, 4227-4233.

[25]   Kronos, private communication. Website: http://www.kronostio2.com/ (accessed: June 27, 2011).

[26]   Nowotny, J.; Bak, T.; Nowotny, M.K.; Sheppard, L.R. Titanium dioxide for solar-hydrogen. I. Functional properties. *Int. J. Hydrogen Energy*, **2007**, *32*, 2609-2629.

[27]   Hu, X.; Li, G.; Yu, J.C. Design, fabrication, and modification of nanostructured semiconductor materials for environmental and energy applications. *Langmuir*, **2010**, *26*, 3031-3039.

[28]   *An assessment of solar energy conversion technologies and research opportunities*, report issued by the Global Climate and Energy Project (GCEP) of Stanford University, Summer **2006**.

[29]   Asahi, R.; Morikawa, T.; Ohwaki, T.; Aoki, K.; Taga, Y. Visible-light photocatalysis in nitrogen-doped titanium oxides. *Science*, **2001**, *293*, 269-271.

[30]   Khan, S.U.M.; Al-Shahry, M.; Ingler Jr, W.B. Efficient photochemical water splitting by a chemically modified n-TiO$_2$. *Science*, **2002**, *297*, 2243-2245.

[31]   Service, R.F. Catalyst Boosts Hopes for Hydrogen Bonanza. *Science*, **2002**, *297*, 2189-2190.

[32]   Osterloh, F.E.; Parkinson, B.A. Recent developments in solar water-splitting photocatalysis. *MRS Bull.*, **2011**, *36*, 17-22.

[33]   Mor, G.K.; Shankar, K.; Paulose, M.; Varghese, O.K.; Grimes, C.A. Enhanced photocleavage of water using titania nanotube arrays. *Nano Lett.*, **2005**, *5*, 191-195.

[34]   Khan, S.U.M.; Sultana, T. Photoresponse of n-TiO$_2$ thin film and nanowire electrodes. *Sol. Energy Mater. Sol. Cells*, **2003**, *76*, 211-221.

[35]   Osterloh, F.E.; Parkinson, B.A. (Eds), Recent developments in solar water-splitting photocatalysis, *MRS Bull.*, **2011**, *36*, pp. 17-55.

[36]   Grünwald, R.; Tributsch, H. Mechanisms of instability in Ru-based dye sensitization solar cells. *J. Phys. Chem. B*, **1997**, *101*, 2564-2575.

[37]   Grätzel, M. Dye-sensitized solar cells. *J. Photochem. Photobiol. C*, **2003**, *4*, 145-153.

[38]   Tributsch, H. Reaction of excited chlorophyll molecules at electrodes and in photosynthesis. *Photochem. Photobiol.*, **1972**, *16*, 261-269.

[39]   Chiba, Y.; Islam, A.; Watanabe, Y.; Komiya, R.; Koide, N.; Han, L. Dye-sensitized solar cells with conversion efficiency of 11.1%. *Jpn. J. Appl. Phys.*, **2006**, *45*, L638-L640.

[40]   Nattestad, A.; Mozer, A.J.; Fischer, M.K.R.; Cheng, Y.-B.; Mishra, A.; Bäuerle, P.; Bach, U. Highly efficient photocathodes for dye-sensitized tandem solar cells. *Nature Mater.*, **2010**, *9*, 31-35.

[41]   Grätzel, M. Solar energy conversion by dye-sensitized photovoltaic cells. *Inorg. Chem.*, **2005**, *44*, 6841-6851.

[42]   Lagref, J.-J.; Nazeeruddin, M.K.; Grätzel, M. Artificial photosynthesis based on dye-sensitized nanocrystalline TiO$_2$ solar cells. *Inorg. Chim. Acta*, **2008**, *361*, 735-745.

[43]   Marquet, P.; Andersson, G.; Snedden, A.; Kloo, L.; Atkin, R. Molecular scale characterization of the titania-dye-solvent interface in dye-sensitized solar cells. *Langmuir*, **2010**, *26*, 9612-9616.

[44]   Schiffmann, F.; VandeVondele, J.; Hutter, J.; Urakawa, A.; Wirz, R.; Baiker, A. An atomistic picture of the regeneration process in dye sensitized solar cells. *Proc. Natl. Acad. Sci. U.S.A.*, **2010**, *107*, 4830-4833.

[45]   Grätzel, M. Sol-gel processed TiO$_2$ films for photovoltaic applications. *J. Sol-Gel Sci. Technol.*, **2001**, *22*, 7-13.

[46]   Martini, I.; Hodak, J.H.; Hartland, G.V. Effect of water on the electron transfer dynamics of 9-anthracenecarboxylic acid bound to TiO$_2$ nanoparticles: Demonstration of the Marcus inverted region. *J. Phys. Chem. B*, **1998**, *102*, 607-614.

[47]   Bauer, C.; Boschloo, G.; Mukhtar, E.; Hagfeldt, A. Electron injection and recombination in Ru(dcbpy)$_2$(NCS)$_2$ sensitized nanostructured ZnO. *J. Phys. Chem. B*, **2001**, *105*, 5585-5588.

[48]   Brabec, C.J. Organic photovoltaics: Technology and market. *Sol. Energy Mater. Sol. Cells*, **2004**, *83*, 273-292.

[49]   Dennler, G.; Scharber, M.C.; Brabec, C.J. Polymer-fullerene bulk-heterojunction solar cells. *Adv. Mater.*, **2009**, *21*, 1323-1338.

[50]   Gaudiana, R. Third-generation photovoltaic technology - The potential for low-cost solar energy conversion. *J. Phys. Chem. Lett.*, **2010**, *1*, 1288-1289.

[51]   Samsung website: http://samsungsdi.com/nextenergy/dssc-solar-cell-battery.jsp (accessed: June27, 2011).

[52]   Kohle, O.; Grätzel, M.; Meyer, A.F.; Meyer, T.B. The photovoltaic stability of bis(isothiocyanato)ruthenium(II)-bis-2,2'-bipyridine-4,4'-dicarboxylic acid and related sensitizers. *Adv. Mater.*, **1997**, *9*, 904-906.

[53]   Figgemeier E.; Hagfeldt, A. Are dye-sensitized nano-structured solar cells stable? An overview of device testing and component analyses. *Int. J. Photoenergy*, **2004**, *6*, 127-140.

[54]   Macht, B.; Turrión, M.; Barkschat, A.; Salvador, P.; Ellmer, K.; Tributsch, H. Patterns of efficiency and degradation in dye sensitization solar cells measured with imaging techniques. *Sol. Energy Mater. Sol. Cells*, **2002**, *73*, 163-173.

[55]   Barkschat, A.; Moehl, T.; Macht, B.; Tributsch, H. The function of TiO₂ with respect to sensitizer stability in nanocrystalline dye solar cells. *Int. J. Photoenergy*, **2008**, Article ID 814951, 13 pp.

[56]   Frost & Sullivan website: http://www.frost.com/ (accessed: June 27, 2011).

[57]   4ᵗʰ International Conference on the Industrialisation of Dye Solar Cells (DSC-IC 2010) website: http://www.dsc-ic.com (accessed: June 27, 2011).

[58]   Kang, S.H.; Choi, S.-H.; Kang, M.-S.; Kim, J.-Y.; Kim, H.-S.; Hyeon, T.; Sung, Y.-E. Nanorod-based dye-sensitized solar cells with improved charge collection efficiency. *Adv. Mater.*, **2008**, *20*, 54-58.

[59]   ISI Web of Knowledge of Thomson Reuters website: http://wokinfo.com/ (accessed: June 27, 2011).

[60]   World Intellectual Property Organization (WIPO) Search Service website: http://www.wipo.int/patentscope (accessed: June 27, 2011).

[61]   Lincot, D. Solution growth of functional zinc oxide thin films and nanostructures. *MRS Bull.*, **2010**, *35*, 778-789.

[62]   Tsoukleris, D.S.; Arabatzis, I.M.; Chatzivasiloglou, E.; Kontos, A.I.; Belessi, V.; Bernard, M.C.; Falaras, P. 2-Ethyl-1-hexanol based screen-printed titania thin films for dye-sensitized solar cells. *Sol. Energy*, **2005**, *79*, 422-430.

[63]   Agarwala, S.; Kevin, M.; Wong, A.S.W.; Peh, C.K.N.; Thavasi, V.; Ho, G.W. Mesophase ordering of TiO₂ film with high surface area and strong light harvesting for dye-sensitized solar cell. *Appl. Mater. Interfaces*, **2010**, *2*, 1844-1850.

[64]   Kallioinen, J.; Benkö, G.; Myllyperkiö, P.; Khriachtchev, L.; Skårman, B.; Wallenberg, R.; Tuomikoski, M.; Korppi-Tommola, J.; Sundström, V.; Yartsev, A.P. Photoinduced ultrafast dynamics of Ru(dcbpy)₂(NCS)₂-sensitized nanocrystalline TiO₂ films: The influence of sample preparation and experimental conditions. *J. Phys. Chem. B*, **2004**, *108*, 6365-6373.

[65]   Nguyen, T.-V.; Lee, H.-C.; Yang, O.-B. The effect of pre-thermal treatment of TiO₂ nano-particles on the performances of dye-sensitized solar cells. *Sol. Energy Mater. Sol. Cells*, **2006**, *90*, 967-981.

[66]   Nazeeruddin, M.K.; Humphry-Baker, R.; Liska, P.; Grätzel, M. Investigation of sensitizer adsorption and the influence of protons on current and voltage of a dye-sensitized nanocrystalline TiO₂ solar cell. *J. Phys. Chem. B*, **2003**, *107*, 8981-8987.

[67]   Baia, L.; Peter, A.; Cosoveanu, V.; Indrea, E.; Baia, M.; Popp, J.; Danciu, V. Synthesis and nanostructural characterization of TiO₂ aerogels for photovoltaic devices. *Thin Solid Films*, **2006**, *511-512*, 512-516.

[68]   Meyer, G.J. Molecular approaches to solar energy conversion with coordination compounds anchored to semiconductor surfaces. *Inorg. Chem.*, **2005**, *44*, 6852-6864.

[69]   Shankar, K.; Basham, J.I.; Allam, N.K.; Varghese, O.K.; Mor, G.K.; Feng, X.; Paulose, M.; Seabold, J.A.; Choi, K.-S.; Grimes, C.A. Recent advances in the use of TiO₂ nanotube and nanowire arrays for oxidative photoelectrochemistry. *J. Phys. Chem. C*, **2009**, *113*, 6327-6359.

[70]   Bwana, N.N. Effects of electrode film modifications on the open-circuit photovoltage in enhanced dye-sensitized solar cells. *J. Nanoparticle Res.*, **2009**, *11*, 1905-1915.

[71]   Bwana, N.N. Comparison of the performances of dye-sensitized solar cells based on different TiO₂ electrodes nanostructures. *J. Nanoparticle Res.*, **2009**, *11*, 1917-1923.

[72]   Shi, Q.-M.; Hou, Y.-B.; Li, Y.; Feng, Z.-H.; Liu, X.-J. Role of TiO₂ nanotube on improvement of performance of hybrid photovoltaic devices. *Chin. Phys. Lett.*, **2009**, *26*, 017202-1-017202-4.

[73]   Hsiao, P.-T.; Wang, K.-P.; Cheng, C.-W.; Teng, H. Nanocrystalline anatase TiO₂ derived from a titanate-directed route for dye-sensitized solar cells. *J. Photochem. Photobiol. A*, **2007**, *188*, 19-24.

[74]   Mor, G.K.; Shankar, K.; Paulose, M.; Varghese, O.K.; Grimes, C.A. Use of highly-ordered TiO₂ nanotube arrays in dye-sensitized solar cells. *Nano Lett.*, **2006**, *39*, 2498-2503.

[75]   Tan, L.K.; Kumar, M.K.; An, W.W.; Gao, H. Transparent, well-aligned TiO₂ nanotube arrays with controllable dimensions on glass substrates for photocatalytic applications. *Appl. Mater. Interfaces*, **2010**, *2*, 498-503.

[76]   Park, N.-G.; van de Lagemaat, J.; Frank, A. J. Comparison of dye-sensitized rutile- and anatase-based TiO₂ solar cells. *J. Phys. Chem. B*, **2000**, *104*, 8989-8994.

[77]   Han, H.; Zan, L.; Zhong, J.; Zhao, X. A novel hybrid nanocrystalline TiO₂ electrode for the dye-sensitized nanocrystalline solar cells. *J. Mater. Sci.*, **2005**, *40*, 4921-4923.

[78]   Chen, D.; Yang, D.; Geng, J.; Zhu, J.; Jiang, Z. Improving visible-light photocatalytic activity of N-doped TiO₂ nanoparticles *via* sensitization by Zn porphyrin. *Appl. Surf. Sci.*, **2008**, *255*, 2879-2884.

[79]   Lim, M.K.; Jang, S.-R.; Vittal, R.; Lee, J.; Kim, K.-J. Linking of N3 dye with C₆₀ through diaminohydrocarbons for enhanced performance of dye-sensitized TiO₂ solar cells. *J. Photochem. Photobiol. A*, **2007**, *190*, 128-134.

[80]   Zhou, W.; Pan, K.; Zhang, L.; Tian, C.; Fu, H. Solar-induced self-assembly of TiO₂–β-cyclodextrin–MWCNT composite wires. *Phys. Chem. Chem. Phys.*, **2009**, *11*, 1713-1718.

[81]   Philippopoulos, A.I.; Terzis, A.; Raptopoulou, C.P.; Catalano, V.J.; Falaras, P. Synthesis, characterization, and sensitizing properties of heteroleptic Ruᴵᴵ complexes based on 2,6-bis(1-pyrazolyl)pyridine and 2,2'-bipyridine-4,4'-dicarboxylic acid ligands. *Eur. J. Inorg. Chem.*, **2007**, 5633-5644.

[82]   Bignozzi, C.A.; Argazzi, R.; Indelli, M.T.; Scandola, F. Design of supramolecular systems for spectral sensitization of semiconductors. *Sol. Energy Mater. Sol. Cells*, **1994**, *32*, 229-244.

[83]   Murai, M.; Furube, A.; Yanagida, M.; Hara, K.; Katoh, R. Near-IR transient absorption spectra of N3 dye as a probe of aggregation on nanocrystalline semiconductor films. *Chem. Phys. Lett.*, **2006**, *423*, 417-421.

[84]   Pérez León, C.; Kador, L.; Peng, B.; Thelakkat, M. Characterization of the adsorption of Ru-bpy dyes on mesoporous TiO₂ Films with UV-Vis, Raman, and FTIR spectroscopies. *J. Phys. Chem. B*, **2006**, *110*, 8723-8730.

[85]   Qu, P.; Meyer, G.J. Proton-controlled electron injection from molecular excited states to the empty states in nanocrystalline TiO₂. *Langmuir*, **2001**, *17*, 6720-6728.

[86]   Hou, Y.-J.; Xie, P.-H.; Zhang, B.-W.; Cao, Y.; Xiao, X.-R.; Wang, W.-B. Influence of the attaching group and substituted position in the photosensitization behavior of ruthenium polypyridyl complexes. *Inorg. Chem.*, **1999**, *38*, 6320-6322.

[87]   Murakoshi, K.; Kano, G.; Wada, Y.; Yanagida, S.; Miyazaki, H.; Matsumoto, M.; Murasawa, S. Importance of binding states between photosensitizing molecules and the TiO₂ surface for efficiency in a dye-sensitized solar cell. *J. Electroanal. Chem.*, **1995**, *396*, 27-34.

[88]   Fan, S.-H.; Wang, K.-Z.; Yang, W.-C. A carbazole-containing difunctional Ruᴵᴵ complex that functions as a pH-induced emission switch and an efficient sensitizer for solar cells. *Eur. J. Inorg. Chem.*, **2009**, 508-518

[89]   Zeng, W.; Cao, Y.; Bai, Y.; Wang, Y.; Shi, Y.; Zhang, M.; Wang, F.; Pan, C.; Wang, P. Efficient dye-sensitized solar cells with an organic photosensitizer featuring orderly conjugated ethylenedioxythiophene and dithienosilole blocks. *Chem. Mater.*, **2010**, *22*, 1915-1925.

[90]   Wu, J.; Lan, Z.; Hao, S.; Li, P.; lin, J.; Huang, M.; Fang, L.; Huang, Y. Progress on the electrolytes for dye-sensitized solar cells. *Pure Appl. Chem.*, **2008**, *80*, 2241-2258.

[91]   Luque, A.; Martí, A.; Nozik, A.J. Solar cells based on quantum dots: Multiple exciton generation and intermediate bands. *MRS Bull.*, **2007**, *32*, 236-241.

[92] Kamat, P.V. Quantum dot solar cells. Semiconductor nanocrystals as light harvesters. *J. Phys. Chem. C*, **2008**, *112*, 18737-18753.

[93] Sambur, J.B.; Riha, S.C.; Choi, D.; Parkinson, B.A. Influence of Surface Chemistry on the Binding and Electronic Coupling of CdSe Quantum Dots to Single Crystal TiO_2 Surfaces. *Langmuir*, **2010**, *26*, 4839-4847.

[94] Acharya, K.P.; Hewa-Kasakarage, N.N.; Alabi, T.R.; Nemitz, I.; Khon, E.; Ullrich, B.; Anzenbacher, P.; Zamkov, M. Synthesis of PbS/TiO_2 colloidal heterostructures for photovoltaic applications. *J. Phys. Chem. C*, **2010**, *114*, 12496-12504.

[95] Noone, K.M.; Ginger, D.S. Doping for speed: Colloidal nanoparticles for thin-film optoelectronics. *ACS Nano*, **2009**, *3*, 261-265.

[96] Lee, H.J.; Chen, P.; Moon, S.-J.; Sauvage, F.; Sivula, K.; Bessho, T.; Gamelin, D.R.; Comte, P.; Zakeeruddin, S.M.; Seok, S.I.; Grätzel, M.; Nazeeruddin, M. K. Regenerative PbS and CdS quantum dot sensitized solar cells with a cobalt complex as hole mediator. *Langmuir*, **2009**, *25*, 7602-7608.

[97] Yu, P.; Zhu, K.; Norman, A.G.; Ferrere, S.; Frank, A.J.; Nozik, A.J. Nanocrystalline TiO_2 solar cells sensitized with InAs quantum dots. *J. Phys. Chem. B*, **2006**, *110*, 25451-25454.

[98] Kang, Q.; Liu, S.; Yang, L.; Cai, Q.; Grimes, C.A. Fabrication of PbS nanoparticle-sensitized TiO_2 nanotube arrays and their photoelectrochemical properties. *Appl. Mater. Interfaces*, **2011**, *3*, 746-749.

[99] Kongkanand, A.; Tvrdy, K.; Takechi, K.; Kuno, M.; Kamat, P.V. Quantum dot solar cells. Tuning photoresponse through size and shape control of CdSe-TiO_2 architecture. *J. Am. Chem. Soc.*, **2008**, *130*, 4007-4015.

[100] Nazeeruddin, M.K.; Kay, A.; Rodicio, I.; Humphry-Baker, R.; Mueller, E.; Liska, P.; Vlachopoulos, N.; Graetzel, M. Conversion of light to electricity by cis-X2bis(2,2'-bipyridyl-4,4'-dicarboxylate)ruthenium(II) charge-transfer sensitizers (X = Cl-, Br-, I-, CN-, and SCN-) on nanocrystalline titanium dioxide electrodes. *J. Am. Chem. Soc.*, **1993**, *115*, 6382-6390.

[101] Greijer Agrell, H.; Lindgren, J.; Hagfeldt, A. Degradation mechanisms in a dye-sensitized solar cell studied by UV–VIS and IR spectroscopy. *Sol. Energy*, **2003**, *75*, 169-180.

[102] Baraton, M.-I. FT-IR surface spectrometry of nanosized particles. In *Handbook of Nanostructured Materials and Nanotechnology*; H.S. Nalwa, Ed.; Academic Press: San Diego, **1999**; pp. 89-153.

[103] Davydov, A.A. *Infrared Spectroscopy of Adsorbed Species on the Surface of Transition Metal Oxides;* Wiley: New York, **1984**.

[104] Wang, Q.; Chen, C.; Zhao, D.; Ma, W.; Zhao, J. Change of adsorption modes of dyes on fluorinated TiO_2 and its effect on photocatalytic degradation of dyes under visible irradiation. *Langmuir*, **2008**, *24*, 7338-7345.

[105] Finnie, K.S.; Bartlett, J.R.; Woolfrey, J.L. Vibrational spectroscopic study of the coordination of (2,2'-bipyridyl-4,4¢-dicarboxylic acid)ruthenium(II) complexes to the surface of nanocrystalline titania. *Langmuir*, **1998**, *14*, 2744-2749.

[106] Hirose, F.; Kuribayashi, K.; Shizaku, M.; Narita, Y. In situ observation of N179 on TiO_2 in dye-sensitized solar cells by IR absorption spectroscopy. *Electrochem. Solid-State Lett.*, **2009**, *12*, B167-B170.

[107] Hirose, F.; Kuribayashi, K.; Shizaku, M.; Narita, Y.; Takahashi, Y.; Kimura, Y.; Niwano, M. Adsorption density control of N179 on TiO_2 electrodes for highly efficient dye-sensitized solar cells. *J. Electrochem. Soc.*, **2009**, *156*, B987-B990.

[108] Hirose, F.; Kuribayashi, K.; Suzuki, T.; Narita, Y.; Kimura, Y.; Niwano, M. UV treatment effect on TiO_2 electrodes in dye-sensitized solar cells with N719 sensitizer investigated by infrared absorption spectroscopy. *Electrochem. Solid-State Lett.*, **2008**, *11*, A109-A111.

[109] Rotzinger, F.P.; Kesselman-Truttmann, J.M.; Hug, S.J.; Shklover, V.; Grätzel, M. Structure and vibrational spectrum of formate and acetate adsorbed from aqueous solution onto the TiO_2 rutile (110) surface. *J. Phys. Chem. B*, **2004**, *108*, 5004-5017.

[110] Wu, W.-C.; Chuang, C.-C.; Lin, J.-L. Bonding geometry and reactivity of methoxy and ethoxy groups adsorbed on powdered TiO_2. *J. Phys. Chem. B*, **2000**, *104*, 8719-8724.

[111] Brownson, J.R.S.; Tejedor-Tejedor, M.I.; Anderson, M.A. FTIR spectroscopy of alcohol and formate interactions with mesoporous TiO_2 surfaces. *J. Phys. Chem. B*, **2006**, *110*, 12494-12499.

[112] Baraton, M.-I. Surface functionalization of semiconducting nanoparticles. In *Encyclopedia of Nanoscience and Nanotechnol-*

[113] Baraton, M.-I.; Merhari, L. Surface chemistry of titanium oxide nanoparticles and its influence on electrical and gas sensing properties. *J. Eur. Ceram. Soc.*, **2004**, *24*, 1399-1404.

[114] Busca, G.; Saussey, H.; Saur, O.; Lavalley, J.-C.; Lorenzelli, V. FT-IR characterization of the surface acidity of different titanium dioxide anatase preparations. *Appl. Catal.*, **1985**, *14*, 245-260.

[115] Primet, M.; Pichat, P.; Mathieu, M.-V. Etude par spectrométrie infrarouge des groupes hydroxyls de l'anatase et du rutile. *C. R. Acad. Sci. Paris, Série B*, **1968**, *267*, 799-802.

[116] Primet, M.; Pichat, P.; Mathieu, M.-V. Infrared study of the surface of titanium dioxides. I. Hydroxyl groups. *J. Phys. Chem.*, **1971**, *75*, 1216-1220.

[117] Primet, M.; Pichat, P.; Mathieu, M.-V. Infrared study of the surface of titanium dioxides. II. Acidic and basic properties. *J. Phys. Chem.*, **1971**, *75*, 1221-1226.

[118] Morterra, C. An infrared spectroscopic study of anatase properties. Part 6: Surface hydration and strong Lewis acidity of pure and sulphate-doped preparations. *J. Chem. Soc., Faraday Trans. 1*, **1988**, *84*, 1617-1637.

[119] Yates, D.J.C. Infrared studies of the surface hydroxyl groups on titanium dioxide, and of the chemisorption of carbon monoxide and carbon dioxide. *J. Phys. Chem.*, **1961**, *65*, 746-753.

[120] Martra, G. Lewis acid and base sites at the surface of microcrystalline TiO_2 anatase: Relationships between surface morphology and chemical behavior. *Appl. Catal. A*, **2000**, *200*, 275-285.

[121] Baraton, M.-I. Surface analysis of semiconducting nanoparticles by FTIR spectroscopy: Application to the evaluation of gas sensing properties. In *Nanocrystalline Metals and Oxides: Selected Properties and Applications*; P. Knauth and J. Schoonman, Eds.; Kluwer Academic Publishers: Boston, **2002**, pp. 165-187.

[122] Tanaka, T.; Kumagai, H.; Hattori, H.; Kudo, M.; Hasegawa, S. Generation of basic sites on TiO_2 by reduction with H_2. *J. Catal.*, **1991**, *127*, 221-226.

[123] Ferretto, L.; Glisenti, A. Surface acidity and basicity of a rutile powder. *Chem. Mater.*, **2003**, *15*, 1181-1188.

[124] Dines, T.J.; Rochester, C.H.; Ward, A.M. Infrared and Raman study of the adsorption of NH_3, pyridine, NO and NO_2 on anatase. *J. Chem. Soc., Faraday Trans.*, **1991**, *87*, 643-651.

[125] Gong, X.-Q.; Selloni, A.; Vittadini, A. Density functional theory study of formic acid adsorption on anatase $TiO_2(001)$: Geometries, energetics, and effects of coverage, hydration, and reconstruction. *J. Phys. Chem. B*, **2006**, *110*, 2804-2811.

[126] Cocks, I.D.; Guo, Q.; Patel, R.; Williams, E.M.; Roman, E.; de Segovia, J.L. The structure of $TiO_2(110)$ (1x1) and (1x2) surfaces with acetic acid adsorption - A PES study. *Surf. Sci.*, **1997**, *377-379*, 135-139.

[127] Kim, K.S.; Barteau, M.A. Structural dependence of the selectivity of formic acid decomposition on faceted titania (001) surfaces. *Langmuir*, **1990**, *6*, 1485-1488.

[128] Xu, C.; Koel, B.E. Adsorption and reaction of CH_3COOH and CD_3COOD on the MgO(100) surface: A Fourier transform infrared and temperature programmed desorption study. *J. Phys. Chem.*, **1995**, *102*, 8158-8166.

[129] Popova, G.Ya.; Andrushkevich, T.V.; Chesalov, Yu.A.; Stoyanov, E.S. In situ FTIR study of the adsorption of formaldehyde, formic acid, and methyl formiate at the surface of TiO_2 (anatase). *Kinet. Catal.*, **2000**, *41*, 805-811.

[130] Busca, G.; Lorenzelli, V. Infrared spectroscopic identification of species of species arising from reactive adsorption of carbon oxides on metal oxide. *Mater. Chem.*, **1982**, *7*, 89-126.

[131] Pei, Z.-F.; Ponec, V. On the intermediates of the acetic acid reactions on oxides: An IR study. *Appl. Surf. Sci.*, **1996**, *103*, 171-182.

[132] Brownson, J.R.S.; Tejedor-Tejedor, M.I.; Anderson, M.A. Photoreactive anatase consolidation characterized by FTIR spectroscopy. *Chem. Mater.*, **2005**, *17*, 6304-6310.

[133] Brownson, J.R.S.; Lee, T.J.; Anderson, M.A. Surface re-esterification and photo sintering of titania xerogel thin films. *Chem. Mater.*, **2005**, *17*, 3025-3030.

[134] Deacon, G.B.; Huber, F.; Phillips, R.J. Diagnosis of the nature of carboxylate coordination from the direction of shifts of carbon-oxygen stretching frequencies. *Inorg. Chim. Acta*, **1985**, *104*, 41-45.

[135] Deacon, G.B.; Phillips, R.J. Relationships between the carbon-oxygen stretching frequencies of carboxylato complexes and the

type of carboxylate coordination. *Coord. Chem. Rev.*, **1980**, *33*, 227-250.

[136]　Chambers, S.A.; Thevuthasan, S.; Kim, Y.J.; Herman, G.S.; Wang, Z.; Tober, E.; Ynzunza, R.; Morais, J.; Peden, C.H.F.; Ferris, K.; Fadley, C.S. Chemisorption geometry of formate on TiO$_2$(110) by photoelectron diffraction. *Chem. Phys. Lett.*, **1997**, *267*, 51-57.

[137]　Vittadini, A.; Selloni, A.; Rotzinger, F.P.; Grätzel, M. Formic acid adsorption on dry and hydrated TiO$_2$ anatase (101) surfaces by DFT calculations. *J. Phys. Chem. B*, **2000**, *104*, 1300-1306.

[138]　Wang, C.-Y.; Groenzin, H.; Shultz, M.J. Comparative study of acetic acid, methanol, and water adsorbed on anatase TiO$_2$ probed by sum frequency generation spectroscopy. *J. Am. Chem. Soc.*, **2005**, *127*, 9736-9744.